

# HUMAN IMPACTS

## by the numbers

Griffin Chure<sup>1</sup>, Rachel A. Banks<sup>2</sup>, Avi Flamholz<sup>2</sup>, Nicholas S. Sarai<sup>3</sup>,  
 Mason Kamb<sup>4</sup>, Ignacio Lopez-Gomez<sup>5</sup>, Tine Valencic<sup>1</sup>,  
 Yinon Bar-On<sup>6</sup>, Ron Milo<sup>6</sup>, Rob Phillips<sup>2,7,\*</sup>

California Institute of Technology, Pasadena, CA, USA, 91125:

1. Department of Applied Physics; 2. Division of Biology and Biological Engineering; 3. Division of Chemistry and Chemical Engineering;

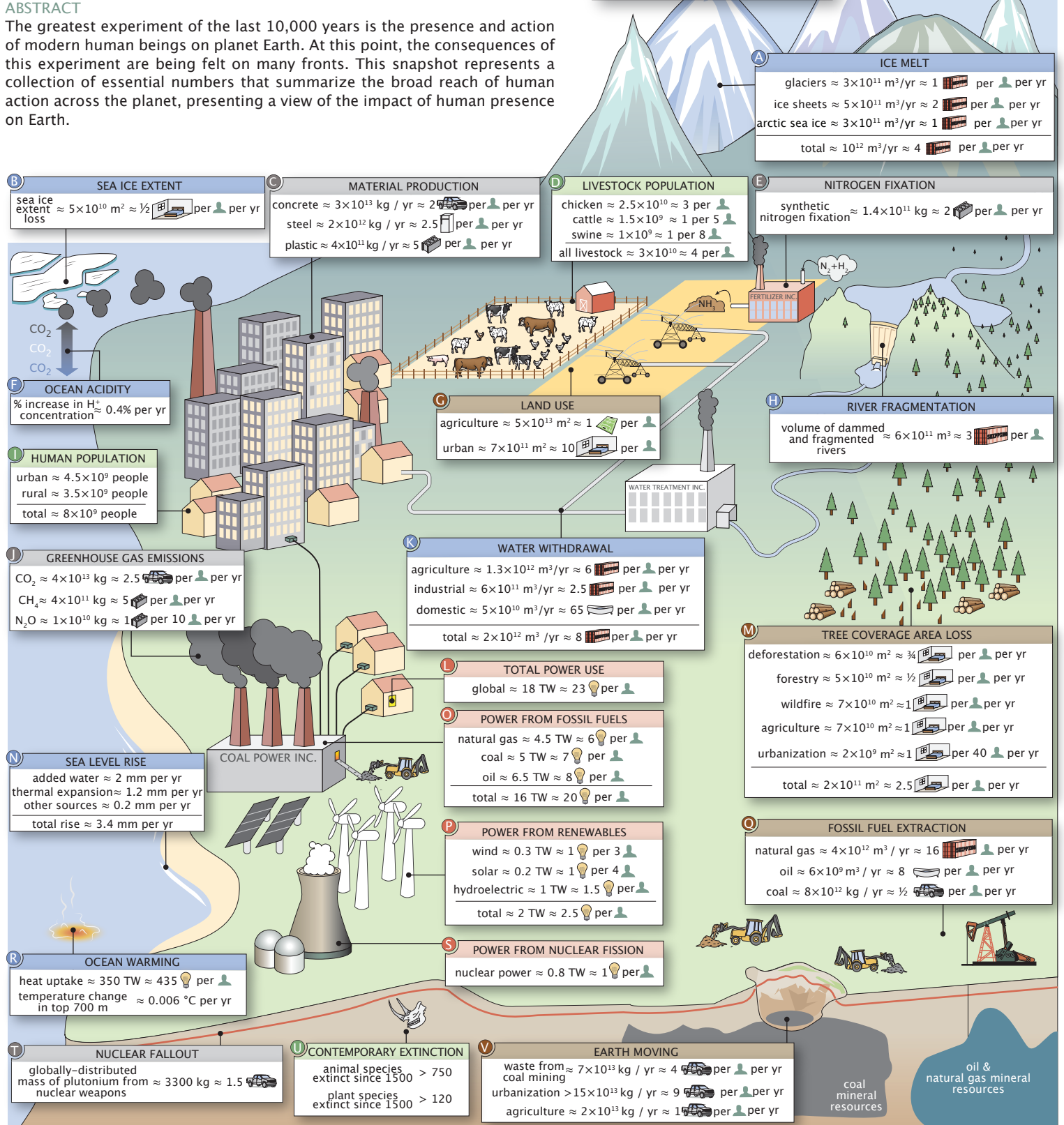
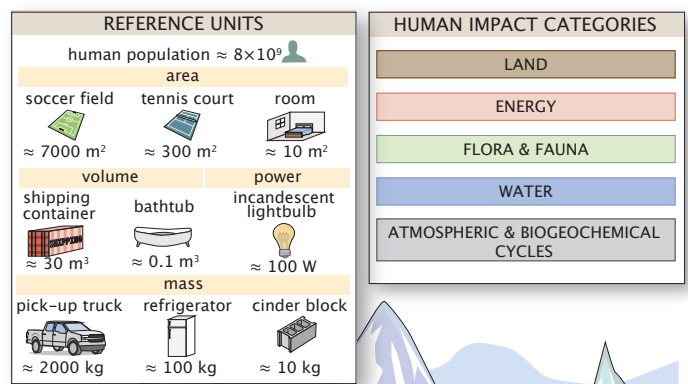
5. Department of Environmental Science and Engineering; 7. Department of Physics;

<sup>4</sup> Chan-Zuckerberg BioHub, San Francisco, CA, 94158

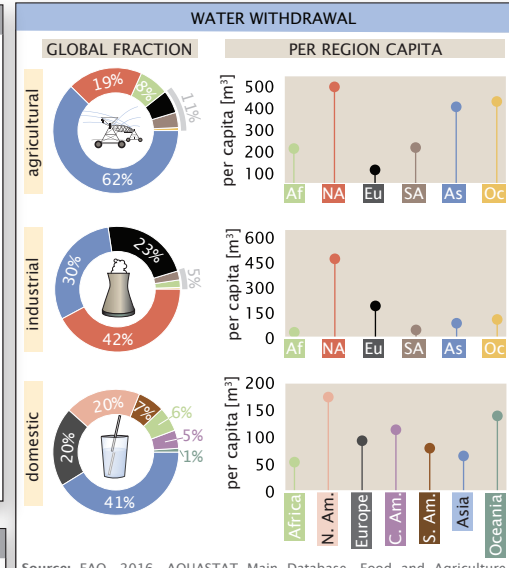
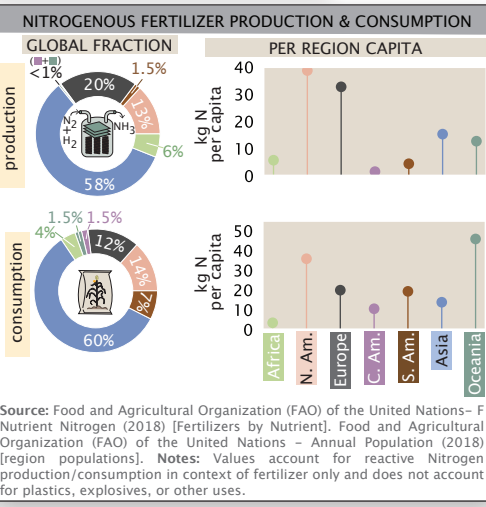
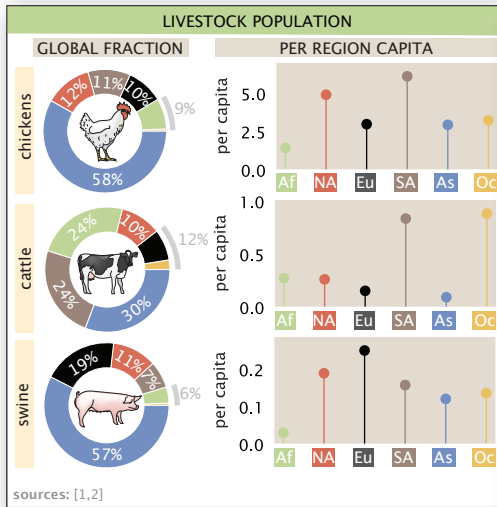
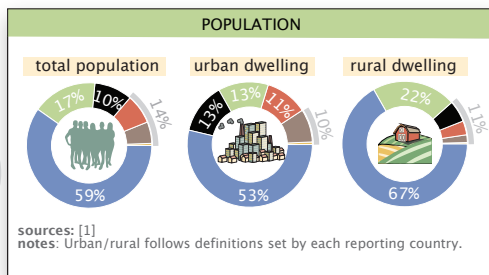
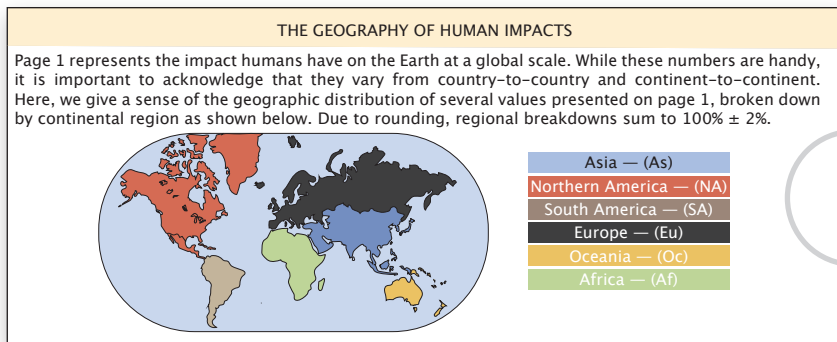
<sup>6</sup> Weizmann Institute of Science, Rehovot 7610001, Israel: Department of Plant and Environmental Sciences

### ABSTRACT

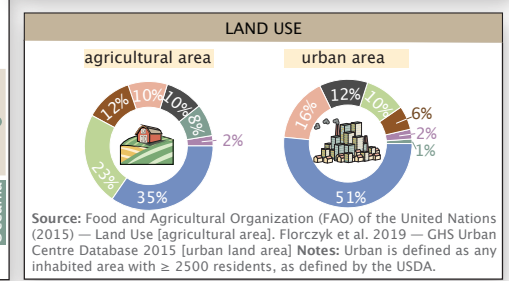
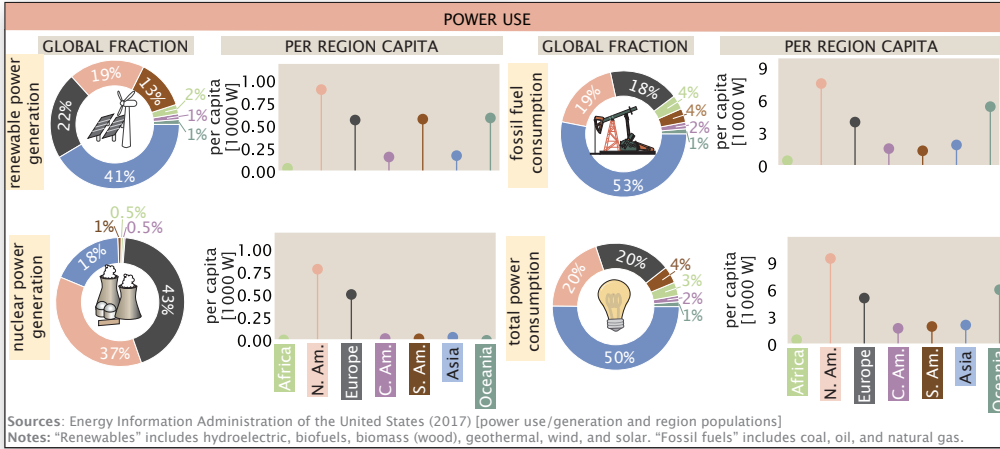
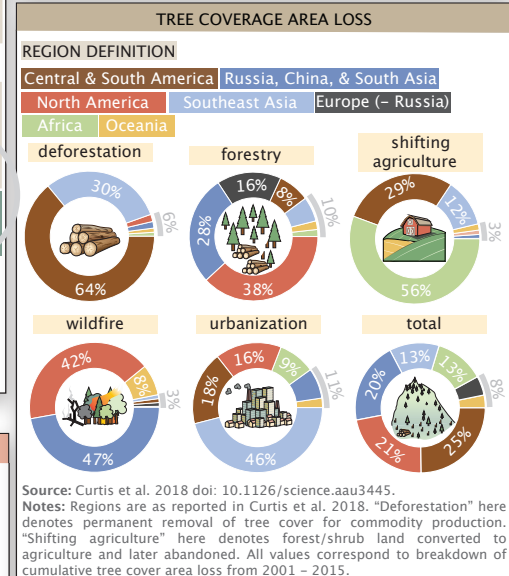
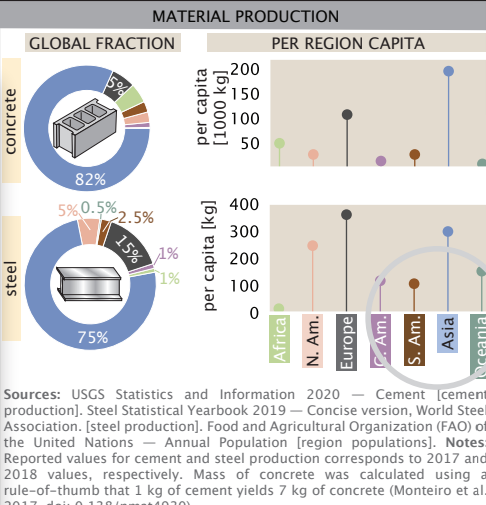
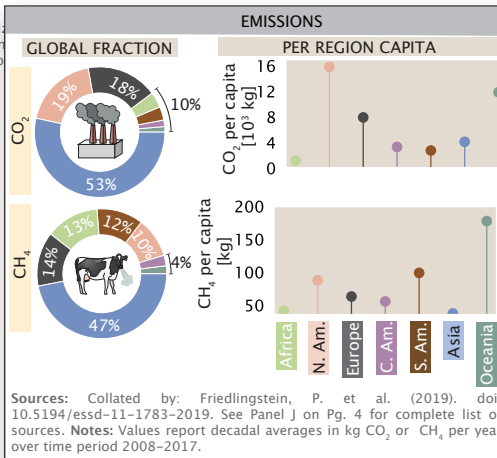
The greatest experiment of the last 10,000 years is the presence and action of modern human beings on planet Earth. At this point, the consequences of this experiment are being felt on many fronts. This snapshot represents a collection of essential numbers that summarize the broad reach of human action across the planet, presenting a view of the impact of human presence on Earth.



# Human Impacts by the Numbers — Impacts by Region



Source: FAO. 2016. AQUASTAT Main Database, Food and Agriculture Organization of the United Nations (FAO). Notes: Values are reported directly from member countries and represent average of 2013–2017 period. Per capita values are computed given population of reporting countries.



## SIZING UP THE ANTHROPOCENE

Much of our understanding of the scales of things is comparative. When we measure lengths, we do so relative to some intuitive distance that provides context. Our aim here is to present some "yardstick" to measure those numbers presented on pages 1 and 2 in a ratiometric form that compares the magnitude of a given human impact to some natural scale for that same quantity. For example, in considering the use of land by humans, a natural dimensionless way to characterize that number is by comparing it to the total land area of our planet, a comparison that yields what we call the "Terra number." Similarly, when we consider the entirety of human-made materials, it is natural to compare this mass to the total biomass on our planet. Here we present twelve key human impacts in this dimensionless form. These numbers describe the solid earth, the atmosphere, the oceans, and human energy use, and we hope that our readers will be emboldened to consider their own favorite examples in a similar dimensionless format. Where appropriate, we reference key values using a [Human Impacts Database](#) number (HuID) accessible via <https://human-impacts.herokuapp.com>. Visit [https://rpgroup.caltech.edu/hi\\_vignettes](https://rpgroup.caltech.edu/hi_vignettes) for more substantial explorations of some of these quantities.

## THE TERRA NUMBER

$$Te = \frac{\text{land area used by humans}}{\text{total land area of Earth}} = \frac{\text{area of farmland and pastures}}{\text{area of Earth}} \approx 0.3$$

The Terra Number reflects the fact that, while we have been constrained to the small fraction of Earth's surface that is land, we have transformed the terrestrial surface to support our dwellings and, much more importantly, our agriculture. Despite being icons of human activity, urban centers occupy between  $6.5$  and  $7.5 \times 10^7 \text{ km}^2$  (HuID: 41339, 39341), a total less than 1% of the terrestrial surface. In contrast, approximately  $50 \text{ million km}^2$  (HuID: 29582) of land on Earth is used either to grow crops or raise livestock. Together, urban and agricultural lands make up  $\approx 30\%$  of Earth's terrestrial surface.

## THE BARNYARD NUMBER

$$By = \frac{\text{mass of terrestrial livestock}}{\text{mass of terrestrial wild animals}} = \frac{\text{mass of cattle, sheep, pigs, chickens}}{\text{mass of elephants, foxes, pelicans}} \approx 30$$

The Barnyard Number focuses another lens onto the massive agricultural transformation of the planet by comparing the total biomass of terrestrial livestock (e.g. cows, chickens, and pigs) to that of terrestrial wild animals (e.g. elephants, foxes, and pelicans) [3]. As a result of agricultural intensification throughout the 20<sup>th</sup> century, livestock now outweigh all wild terrestrial animals by a factor of  $\approx 30$ . While poultry make up the vast majority of terrestrial livestock ( $\approx 25$  billion individuals, HuID: 94934), they represent a small proportion of livestock biomass. Despite a smaller population of  $\approx 1.5$  billion (HuID: 92006), cattle dominate livestock biomass with a total weight of  $\approx 1.5 \times 10^{12} \text{ kg}$ .

## THE RIVER NUMBER

$$Rv = \frac{\text{river volume controlled by humans}}{\text{free-flowing river volume}} = \frac{\text{volume of rivers under human control}}{\text{volume of free-flowing rivers}} \approx 1$$

Humans have harnessed water from rivers for irrigation, flood control, and generation of hydroelectric power. Harnessing this water, however, requires damming the river – thus interrupting its flow and altering the riverine ecosystem. The River Number quantifies the scale of human interference in river flow by relating the volume of river systems under human control (primarily due to damming) to that of free-flowing rivers. Globally, approximately equal volumes of river water are free flowing ( $\approx 6 \times 10^{11} \text{ m}^3$ , [6] HuID: 55718) as are under direct human control, such as through dams and reservoirs or man-made channels ( $\approx 6 \times 10^{11} \text{ m}^3$ , HuID: 61661). Approximately 50% of global free-flowing river volume is within the Amazon river alone.

THE CO<sub>2</sub> NUMBER

$$CO_2 = \frac{\text{annual mass of anthropogenic CO}_2}{\text{annual mass of naturally removed CO}_2} = \frac{\text{mass of CO}_2 from fossil fuel extraction}}{\text{mass of CO}_2 removed by plants}} \approx 2$$

The CO<sub>2</sub> Number compares the annual amount of human-caused CO<sub>2</sub> emissions to the mass of CO<sub>2</sub> naturally removed from the atmosphere each year. There are many climate-related consequences of increasing CO<sub>2</sub> emissions. Beyond accelerating climate change,  $\approx 25\%$  of CO<sub>2</sub> released into the atmosphere is absorbed by the oceans, making them appreciably more acidic over time. In recent years, human activities, including burning fossil fuels and making concrete, have led to the release of  $\approx 4 \times 10^{13} \text{ kg}$  of CO<sub>2</sub> (HuID: 54608, 24789) into the atmosphere each year. While many natural processes like volcanoes and wildfires release CO<sub>2</sub>, they are generally accompanied by corresponding sinks that remove even more CO<sub>2</sub>, like plant photosynthesis. Once all natural processes have been accounted for, a net natural sink of  $\approx 2 \times 10^{13} \text{ kg}$  of CO<sub>2</sub> per year remains (HuID: 52670). Thus, the CO<sub>2</sub> number quantifies the extent to which human emissions outpace the natural removal of CO<sub>2</sub>.

## THE ANTHROPOMASS NUMBER

$$An = \frac{\text{total anthropomass}}{\text{total biomass}} = \frac{\text{mass of human-made materials}}{\text{mass of plants and animals}} \approx 1$$

The Anthropomass Number takes stock of our material production by comparing the total quantity of human-made materials to the entirety of the biomass on planet Earth. Around 2020, total human made materials added up to the same mass as the total biomass dry weight ( $\approx 1.1 \text{ Tt}$  [1]). Concretes and aggregates (such as gravel) dominate the anthropomass, with bricks and asphalt coming in a distant second. Though around us everywhere, plastics and metals constitute less than 10% of total anthropomass. The total anthropomass budget amounts to a dizzying  $\approx 10^{15} \text{ kg}$  of human made mass, or about 20 African bush elephants, per person on the planet.

## THE EXTINCTION NUMBER

$$Ex = \frac{\text{number of known animal extinctions}}{\text{number of expected natural animal extinctions}} = \frac{\text{number of species lost}}{\text{number of species that would have gone extinct}} > 10$$

Over the past 500 years, far more animal species have gone extinct than would be expected due to natural processes. Since 1500, at least 760 animal species have gone extinct (HuID: 44641). Recent estimates of ancient rates of animal extinction predict that tenfold fewer ( $\approx 50$ ) species would have gone extinct over the same period in the absence of humans [2]. It's important to emphasize that these data are incomplete and reflect only a fraction of species that have been assessed for conservation status. The Extinction Number therefore represents a lower bound on the degree of modern species loss, with the true value likely being much higher.

## THE DEFORESTATION NUMBER

$$Df = \frac{\text{annual forest loss from human action}}{\text{annual forest loss from wildfire}} \approx \frac{\text{volume of logs cut}}{\text{volume of trees burned}} \approx 2$$

The Deforestation Number reflects that humans intentionally deforest and disrupt forested land at twice the rate of wildfires, some of which are also caused by humans. This human-caused forest loss is due to commodity-driven deforestation ( $\approx 6 \times 10^{10} \text{ m}^2$ , HuID: 38352), forestry ( $\approx 5 \times 10^{10} \text{ m}^2$ , HuID: 38352), and shifting forest land to agriculture ( $\approx 7.5 \times 10^{10} \text{ m}^2$ , HuID: 24388). Expansion of urban areas accounts for  $< 1\%$  of the total annual forest loss (HuID: 19429). In total,  $\approx 15 \times 10^{10} \text{ m}^2$  of forest is lost annually due to intentional human action, whereas wildfires (both naturally sparked and those caused by humans) account for  $\approx 7 \times 10^{10} \text{ m}^2$  annually (HuID: 92221).

## THE NIAGARA NUMBER

$$Ni = \frac{\text{daily water volume used by humans}}{\text{Niagara Falls daily discharge volume}} \approx \frac{\text{volume of water used}}{\text{volume of waterfall}} \approx 30$$

The Niagara Number captures the magnitude of human water usage relative to the scale of Niagara Falls, the largest waterfall in North America by discharge (volumetric flow rate). Agriculture once again defines this aspect of the human interaction with the Earth system as it uses  $\approx 1.5 \times 10^{12} \text{ m}^3$  (HuID: 43593) of water annually, accounting for the majority of human water usage. Water used for industrial purposes, including cooling thermoelectric plants amounts to  $5.9 \times 10^{11} \text{ m}^3 / \text{yr}$  (HuID: 27142), and domestic use is  $\approx 6 \times 10^{10} \text{ m}^3 / \text{yr}$  (HuID: 69424). In total, human water annual water withdrawal is  $\approx 30$  times the volume that flows over the Niagara Falls in a year [4] (National Water Information System, 2020, U.S.G.S.) and is comparable to  $\frac{1}{3}$  the yearly discharge of the Amazon river [5].

## THE NITROGEN NUMBER

$$N_2 = \frac{\text{mass of N}_2 \text{ fixed via the Haber-Bosch Process}}{\text{mass of N}_2 \text{ fixed biologically}} \approx \frac{\text{mass of NH}_3 produced}{\text{mass of NH}_3 produced by plants}} \approx 1$$

Though molecular nitrogen (N<sub>2</sub>) makes up nearly 80% of our atmosphere, it must be converted into a more reactive form like ammonia (NH<sub>3</sub>), a primary ingredient in fertilizer, in order for most plants to utilize it. Deemed the "detonator of the population explosion" [8], the 1910 development of the Haber-Bosch process for industrial synthesis of NH<sub>3</sub> from N<sub>2</sub> was critical for supporting the agricultural needs of a growing human population and for supplying NH<sub>3</sub> for chemical and explosive synthesis. The Nitrogen Number reveals that humans synthesize as much reactive nitrogen industrially ( $\approx 1.4 \times 10^{11} \text{ kg per year}$ , HuID: 61614, 60580) as is synthesized by nitrogen-fixing microbes in terrestrial ecosystems ( $\approx 1 \times 10^{11} \text{ kg per year}$ , HuID: 15205). Beyond influencing the balance of reactive nitrogen in the environment, the Haber-Bosch process uses a sizable amount of energy and contributes significantly to global CO<sub>2</sub> emissions.

THE CH<sub>4</sub> NUMBER

$$Me = \frac{\text{annual mass of anthropogenic CH}_4}{\text{annual mass of natural CH}_4} = \frac{\text{mass of CH}_4 from fossil fuel extraction}}{\text{mass of CH}_4 from natural sources}} \approx 1$$

While CO<sub>2</sub> is the most often discussed greenhouse gas, human activities also release substantial amounts of methane (CH<sub>4</sub>), an even more potent greenhouse gas than CO<sub>2</sub>. The CH<sub>4</sub> Number compares human methane emissions to all natural sources of methane. Anthropogenic emissions, resulting from fossil fuel extraction, ruminant livestock (mostly cows), rice cultivation, and other sources total  $\approx 3 - 4 \times 10^9 \text{ kg per year}$  (HuID: 96837). Natural emissions of CH<sub>4</sub>, stemming mostly from wetlands and other anaerobic environments, produce a comparable amount ( $2 - 4 \times 10^9 \text{ kg per year}$ ) to anthropogenic emissions (HuID: 56405). There is substantial uncertainty regarding the magnitude of both natural and anthropogenic methane emissions, on the order of up to  $1 \times 10^9 \text{ kg/year}$  in the anthropogenic case and  $2 \times 10^9 \text{ kg/year}$  in the natural case, due to difficulties in accounting for different sources and some discrepancies between bottom-up accounting and atmospheric modeling approaches.

## THE SOLAR NUMBER

$$Su = \frac{\text{annual human power usage}}{\text{annual incident solar power}} \approx \frac{\text{power used by humans}}{\text{power from the sun}} \approx 0.0001$$

While humans derive biological energy from food, we derive mechanical and electrical power from various fuel sources like coal, oil, natural gas, and fissile nuclear material. Current global human power usage amounts to an enormous 18 terawatts, a number which has been increasing steadily over the last 200 years. The Solar Number puts the 18 TW power consumption of human activities (HuID: 31373; 85317) in relief by comparing it to the power incident on our planet from the sun, which represents a power source roughly 10,000 times greater than our current demands. Of course, it is unlikely that we could ever harness 100% of solar energy incident on our planet, but capturing even 1% of this energy would be sufficient to produce 100 times more power than we currently use.

[1] Elhacham, et al. 2020, in press. [2] Ceballos et al. 2015 doi:10.1126/sciadv.1400253. [3] Bar-On, Y.M. et al. 2018 doi:10.1073/pnas.1711842115 [4] National Water Information System, 2020, U.S.G.S. [5] Transboundary River Basin Overview – Amazon, 2015, AQUASTAT. [6] Grill et al. doi: 10.1038/s41586-019-1111-9. [7] Svititski et al. 2005, doi:10.1126/science.1109454. [8] Smil 1999, doi: 10.1038/22672

# Human Impacts by the Numbers — Supporting Information

**About:** Here, we present citations and notes corresponding to each quantity assessed here. Each value presented on page 1 is assigned a Human Impacts Database identifier (HuID), accessible via <https://human-impacts.herokuapp.com>. When possible, primary data sources have been collated and stored as files in comma-separated-value (csv) format on the GitHub repository associated with this snapshot, accessible via DOI: XXXXXX and [https://github.com/rpgroup-pboc/human\\_impacts](https://github.com/rpgroup-pboc/human_impacts)

<b>A ANNUAL ICE MELT</b> $\text{glaciers} = (3.0 \pm 1.2) \times 10^{11} \text{ m}^3 / \text{yr}$ <span style="float: right;">HuID: 32459</span> <b>Data Source(s):</b> Intergovernmental Panel on Climate Change (IPCC) 2019 Special Report on the Ocean and Cryosphere in a Changing Climate. Table 2.A.1 on pp. 199–202. <b>Notes:</b> Value corresponds to the trend of annual glacial ice mass loss from major glaciated regions (2006–2015) based on aggregation of observation methods (original data source: Zemp et al. 2019, DOI:10.1038/s41586-019-1071-0) with satellite gravimetric observations (original data source: Wouters et al. 2019, DOI:10.3389/feart.2019.00096). Water volume loss was calculated from ice mass loss assuming a standard pure ice density of 920 kg / m <sup>3</sup> . Uncertainty represents a 95% confidence interval calculated from standard error propagation of the 95% confidence intervals reported in the original sources assuming them to be independent.	<b>F OCEAN ACIDIFICATION</b> $\text{surface ocean } [\text{H}^+] \approx 0.2 \text{ parts per billion}$ <span style="float: right;">HuID: 90472</span> annual change in $[\text{H}^+] = 0.36 \pm 0.03 \%$ <span style="float: right;">HuID: 19394</span> <b>Data Source(s):</b> Figures 1–2 of European Environment Agency report CLIM 043 (2020). Original data source of the report is “Global Mean Sea Water pH” from Copernicus Marine Environment Monitoring Service. <b>Notes:</b> Reported value is calculated from the global average annual change in pH over years 1985–2018. The average oceanic pH was $\approx 8.057$ in 2018 and decreases annually by $\approx 0.002$ units, giving a change in $[\text{H}^+]$ of roughly $10^{-8.056} - 10^{-8.057} \approx 4 \times 10^{-11} \text{ mol/L}$ or about 4% of the global average. $[\text{H}^+]$ is calculated as $10^{-\text{pH}} \approx 10^{-8} \text{ mol/L}$ or 0.2 parts per billion (ppb) which is calculated by noting that $[\text{H}_2\text{O}] \approx 55 \text{ mol / L}$ . Uncertainty for annual change is the standard error of the mean.
$\text{ice sheets} = (4.7 \pm 0.4) \times 10^{11} \text{ m}^3 / \text{yr}$ <span style="float: right;">HuID: 95798, 93137</span> <b>Data Source(s):</b> D. N. Wiese et al. 2019 JPL GRACE and GRACE-FO Mascon Ocean, Ice, and Hydrology Equivalent HDR Water Height RL06M CRI Filtered Version 2.0, Ver. 2.0, PO.DAAC, CA, USA. Dataset accessed [2020-Aug-10]. DOI: 10.5067/TEM-SC-3MJ62 <b>Notes:</b> Value corresponds to the trends of combined annual ice mass loss from the Greenland and Antarctic Ice Sheets (2002–2020) measured by satellite gravimetry. Water volume loss was calculated from ice mass loss assuming a standard pure ice density of 920 kg / m <sup>3</sup> . Uncertainty represents one standard deviation and considers only propagation of monthly uncertainties in measurement. $\text{Arctic sea ice} = (3.0 \pm 1.0) \times 10^{11} \text{ m}^3 / \text{yr}$ <span style="float: right;">HuID: 89520</span> <b>Data Source(s):</b> PIOMAS Arctic Sea Ice Volume Reanalysis, Figure 1 of webpage as of October 31, 2020. Original method source: Schweiger et al. 2011, DOI:10.1029/2011JC007084 <b>Notes:</b> Value reported corresponds to the trend of annual volume loss from Arctic sea ice (1979–2020). The uncertainty in the trend represents the range in trends calculated from three ice volume determination methods.	<b>G LAND USE</b> $\text{agricultural} \approx 5 \times 10^{13} \text{ m}^2$ <span style="float: right;">HuID: 29582</span> <b>Data Source(s):</b> Food and Agriculture Organization (FAO) of the United Nations Statistical Database (2020) — Land Use. <b>Notes:</b> Agricultural land is defined as all land that is under agricultural management including pastures, meadows, permanent crops, temporary crops, land under fallow, and land under agricultural structures (such as barns). Reported value corresponds to 2017 estimates by FAO. $\text{urban} \approx (6 - 8) \times 10^{11} \text{ m}^2$ <span style="float: right;">HuID: 41339, 39341</span> <b>Data Source(s):</b> Florczyk et al. 2019 ( <a href="https://tinyurl.com/yxxggtl">https://tinyurl.com/yxxggtl</a> ) and Table 3 of Liu et al. 2018 DOI: 10.1016/j.rse.2018.02.055. <b>Notes:</b> Urban land area is determined from satellite imagery. An area is determined to be “urban” if the total population is greater than 5,000 and has a minimum population density of 300 people per km <sup>2</sup> . Reported value gives the range of recent measurements of $\approx 6.5 \times 10^{11} \text{ m}^2$ (2015) and $\approx (7.5 \pm 1.5) \times 10^{11} \text{ m}^2$ (2010) from Florczyk et al. 2019 and Liu et al. 2018, respectively.
<b>B SEA ICE EXTENT</b> $\text{extent loss at yearly maximum cover (September)} \approx 8.4 \times 10^{10} \text{ m}^2 / \text{yr}$ <span style="float: right;">HuID: 33993</span> $\text{extent loss at yearly minimum cover (March)} \approx 4.0 \times 10^{10} \text{ m}^2 / \text{yr}$ <span style="float: right;">HuID: 87741</span> $\text{average annual extent loss} = 5.5 \pm 0.2 \times 10^{10} \text{ m}^2 / \text{yr}$ <span style="float: right;">HuID: 70818</span> <b>Data Source(s):</b> Comiso et al. 2017, DOI:10.1002/2017JC012768. Fetterer et al. 2017, updated daily. Sea Ice Index, Version 3, [Sea_Ice_Index_Monthly_Data_with_Statistics_G02135_v3.0.xlsx], Boulder, Colorado USA. NSIDC: National Snow and Ice Data Center, DOI:10.7265/NSK072F8, [Accessed 2020-Oct-19]. <b>Notes:</b> Sea ice extent refers to the area of the sea with > 15% ice coverage. Annual value corresponds to the linear trend of annually averaged Arctic sea ice extent from 1979–2015 (Comiso et al 2017) calculated from four different methods. This is in good agreement with the linear trend of annual extent loss calculated by averaging over every month in a given year ( $5.5 \times 10^{10} \text{ m}^2 / \text{yr}$ HuID: 66277). The minimum cover extent loss corresponds to the linear trend of Arctic sea ice extent in September from 1979–2020 and the maximum cover extent loss corresponds to the linear trend of sea ice extent in March from 1979–2020. The Antarctic sea ice extent trend is not shown because a significant long-term trend over the satellite observation period is not observed and short-term trends are not yet attributable.	<b>H RIVER FRAGMENTATION</b> $\text{global fragmented river volume} \approx 6 \times 10^{11} \text{ m}^3$ <span style="float: right;">HuID: 61661</span> <b>Data Source(s):</b> Grill et al. 2019 DOI: 10.1038/s41586-019-1111-9. <b>Notes:</b> Value corresponds to the water volume contained in rivers that fall below the connectivity threshold required to classify them as free-flowing. Value considers only global rivers with upstream catchment areas greater than 10 km <sup>2</sup> or discharge volumes greater than 0.1 m <sup>3</sup> per second. The ratio of global river volume in disrupted rivers to free-flowing rivers is approximately 0.9. The exact value depends on the cutoff used to define a “free-flowing” river. We direct the reader to the source for thorough detail.
<b>C MATERIAL PRODUCTION</b> $\text{concrete production} = (2 - 3) \times 10^{13} \text{ kg / yr}$ <span style="float: right;">HuID: 25488, 81346</span> <b>Data Source(s):</b> United States Geological Survey (USGS), Mineral Commodity Summaries 2020, pp. 42–43, DOI:10.3133/mcs2020. Miller et al. 2016, Table 1, DOI:10.1088/1748-9326/11/7/074029. Monteiro et al. 2017, DOI:10.1038/nmat4930. <b>Notes:</b> Concrete is formed when aggregate material is bonded together by hydrated cement. The USGS reports the mass of cement produced in 2019 as $4.1 \times 10^{12} \text{ kg}$ in 2019. As most cement is used to form concrete, cement production can be used to estimate concrete mass using a multiplicative conversion factor of 7 (Monteiro et al.). Miller et al. report that the cement, aggregate and water used in concrete in 2012 sum to $2.3 \times 10^{13} \text{ kg}$ . $\text{steel production} = 1.9 \times 10^{12} \text{ kg / yr}$ <span style="float: right;">HuID: 51453, 44894</span> <b>Data Source(s):</b> United States Geological Survey (USGS), Mineral Commodity Summaries 2020, pp. 82–83, DOI:10.3133/mcs2020. World Steel Association, World Steel in Figures 2020, p. 6. <b>Notes:</b> Crude steel includes stainless steels, carbon steels, and other alloys. The USGS reports the mass of crude steel produced in 2019 as 1900 megatonnes (Mt). The World Steel Association reports a production value of 1869 Mt in 2019. $\text{plastic production} \approx 4 \times 10^{11} \text{ kg / yr}$ <span style="float: right;">HuID: 97241</span> <b>Data Source(s):</b> Geyer et al. 2017, Table S1, DOI:10.1126/sciadv.1700782. <b>Notes:</b> Value represents the approximate sum total global production of plastic fibers and plastic resin during the calendar year of 2015. Notably, comprehensive data about global plastic production is sorely lacking. Geyer et al. draw data from various industry groups to estimate total production of different polymers and additives. Some of the underlying data is not publicly available, and data from financially-interested parties is inherently suspect.	<b>I HUMAN POPULATION</b> $\text{urban-dwelling fraction of population} \approx 55\%$ <span style="float: right;">HuID: 93995</span> $\text{total population} \approx 7.6 \times 10^9$ <span style="float: right;">HuID: 85255</span> <b>Data Source(s):</b> Food and Agricultural Organization (FAO) of the United Nations Report on Annual Population, 2019. <b>Notes:</b> Value for total population in 2018 comes from a combination of direct population reports from country governments as well as inferences of underreported or missing data. The definition of “urban” differs between countries and the data does not distinguish between urban and suburban populations despite substantive differences between these land uses. As explained by the United Nations population division, “When the definition used in the latest census was not the same as in previous censuses, the data were adjusted whenever possible so as to maintain consistency.” Rural population is computed from this fraction along with the total human population, implying that the total population is composed only of “urban” and “rural” communities.
<b>D LIVESTOCK POPULATION</b> $\text{chicken standing population} \approx 2.5 \times 10^{10}$ <span style="float: right;">HuID: 94934</span> $\text{cattle standing population} \approx 1.5 \times 10^9$ <span style="float: right;">HuID: 92006</span> $\text{swine standing population} \approx 1 \times 10^9$ <span style="float: right;">HuID: 21368</span> $\text{all livestock standing population} \approx 3 \times 10^{10}$ <span style="float: right;">HuID: 15765</span> <b>Data Source(s):</b> Food and Agriculture Organization (FAO) of the United Nations Statistical Database (2020) — Live Animals. <b>Notes:</b> Counts correspond to the estimated standing populations in 2018. Values are reported directly by countries, yet the FAO uses non-governmental statistical sources to address uncertainty and missing (non-reported) data. Reported values are therefore approximations.	<b>J GREENHOUSE GAS EMISSIONS</b> $\text{anthropogenic CO}_2 = (4.25 \pm 0.33) \times 10^{13} \text{ kg CO}_2 / \text{yr}$ <span style="float: right;">HuID: 24789, 54608, 98043</span> <b>Data Source(s):</b> Table 6 of Friedlingstein et al. 2019, DOI: 10.5194/essd-11-1783-2019. Original data sources relevant to this study compiled in Friedlingstein et al.: 1) Gilfillan et al. <a href="https://energy.appstate.edu/CDIAC">https://energy.appstate.edu/CDIAC</a> 2) Average of two bookkeeping models: Houghton and Nassikas 2017 DOI: 10.1002/2016GB005546; Hansis et al. 2015 DOI: 10.1002/2014GB004997) Dlugokencky and Tans, NOAA/GML <a href="https://www.esrl.noaa.gov/gmd/ccgg/trends/">https://www.esrl.noaa.gov/gmd/ccgg/trends/</a> . <b>Notes:</b> Value corresponds to total CO <sub>2</sub> emissions from fossil fuel combustion, industry (predominantly cement production), and land-use change during calendar year 2018. Changes to land can lead to CO <sub>2</sub> emissions indirectly. When forests are harvested, for example, CO <sub>2</sub> that would otherwise be removed by photosynthesis remains in the atmosphere. In 2018, $1.88 \times 10^{12} \text{ kg CO}_2 / \text{yr}$ accumulated in the atmosphere, reflecting the balance of emissions and CO <sub>2</sub> uptake by plants and oceans. Uncertainty corresponds to one standard deviation.
<b>E NITROGEN FIXATION</b> $\text{annual mass of fixed nitrogen} \approx 1.4 \times 10^{11} \text{ kg / yr}$ <span style="float: right;">HuID: 60580, 61614</span> <b>Data Source(s):</b> United States Geological Survey (USGS), Mineral Commodity Summaries 2020, pp. 116–117, DOI:10.3133/mcs2020. International Fertilizer Association (IFA) Statistical Database (2019) — Ammonia Production & Trade Tables by Region. Smith et al. 2020, DOI: 10.1039/c9ee02873k. <b>Notes:</b> Ammonia (NH <sub>3</sub> ) produced globally is compiled by the USGS and IFA from major factories that report output. The USGS reports the approximate mass of nitrogen in ammonia produced in 2018 as $1.44 \times 10^{11} \text{ kg}$ and the International Fertilizer Association reports a production value of $1.46 \times 10^{11} \text{ kg}$ in 2018. Both sources compile nearly all of this mass is produced by the Haber-Bosch process (>96%, Smith et al. 2020). In the United States most of this mass is used for fertilizer, with the remainder being used to synthesize nitrogen-containing chemicals including explosives, plastics, and pharmaceuticals (~ 88%, USGS Mineral Commodity Summaries 2020).	<b>K WATER WITHDRAWAL</b> $\text{agricultural withdrawal} = 1.3 \times 10^{12} \text{ m}^3 / \text{yr}$ <span style="float: right;">HuID: 84545, 43593, 95345</span> $\text{industrial withdrawal} = 5.9 \times 10^{11} \text{ m}^3 / \text{yr}$ <span style="float: right;">HuID: 27142</span> $\text{domestic withdrawal} = 5.4 \times 10^{10} \text{ m}^3 / \text{yr}$ <span style="float: right;">HuID: 69424</span> $\text{total withdrawal} = (1.7 - 2.2) \times 10^{12} \text{ m}^3 / \text{yr}$ <span style="float: right;">HuID: 27342, 68004</span> <b>Data Source(s):</b> Figure 1 of Qin et al. 2019. DOI: 10.1038/s41893-019-0294-2. AQUASTAT Main Database, Food and Agriculture Organization of the United Nations <b>Notes:</b> Agricultural and total withdrawal include one value from Qin et al. (who reports “consumption”) and one value from the AQUASTAT database. Industrial water withdrawal is from AQUASTAT and domestic withdrawal value is from Qin et al. Values in AQUASTAT are self-reported by countries and have missing values from some countries, probably accounting for a few percent underreporting. All values represent water withdrawals. For agricultural and domestic, water withdrawal is assumed to be the same as water consumption, which is reported in Qin et al.

# Human Impacts by the Numbers — Supporting Information (Continued)

L	TOTAL POWER USE	
	global power use = $17 - 18 \text{ TW}$	<a href="#">HuID: 31373, 85317</a>
	<b>Data Source(s):</b> bp Statistical Review of World Energy, 2020; U.S. Energy Information Administration, 2020. <b>Notes:</b> Value represents the sum of total primary energy consumed from oil, natural gas, coal, and nuclear energy and electricity generated by hydroelectric and other renewables. Value is calculated using annual primary energy consumption as reported in data sources assuming uniform use throughout a year, yielding $\approx 17 - 18 \text{ TW}$ .	
M	TREE COVERAGE AREA LOSS	
	commodity-driven deforestation = $(5.7 \pm 1.1) \times 10^{10} \text{ m}^2 / \text{yr}$	<a href="#">HuID: 96098</a>
	forestry = $(5.4 \pm 0.8) \times 10^{10} \text{ m}^2 / \text{yr}$	<a href="#">HuID: 38352</a>
	urbanization = $(2 \pm 1) \times 10^9 \text{ m}^2 / \text{yr}$	<a href="#">HuID: 19429</a>
	shifting agriculture = $(7.5 \pm 0.9) \times 10^{10} \text{ m}^2 / \text{yr}$	<a href="#">HuID: 24388</a>
	wildfire = $(7.2 \pm 1.3) \times 10^{10} \text{ m}^2 / \text{yr}$	<a href="#">HuID: 92221</a>
	<b>Data Source(s):</b> Table 1 of Curtis et al. 2018 DOI: <a href="https://doi.org/10.1126/science.aau3445">10.1126/science.aau3445</a> . Hansen et al. 2013 DOI: <a href="https://doi.org/10.1126/science.1244693">10.1126/science.1244693</a> . Global Forest Watch, 2020. Reported values in source correspond to total loss from 2001 – 2015. Values given are averages over this 15 year window. <b>Notes:</b> Commodity-driven deforestation is “long-term, permanent, conversion of forest and shrubland to a non-forest land use such as agriculture, mining, or energy infrastructure.” Forestry is defined as large-scale operations occurring within managed forests and tree plantations with evidence of forest regrowth in subsequent years. Urbanization converts forest and shrubland for the expansion and intensification of existing urban centers. Disruption due to “shifting agriculture” is defined as “small- to medium-scale forest and shrubland conversion for agriculture that is later abandoned and followed by subsequent forest regrowth”. Disruption due to wildfire is “large-scale forest loss resulting from the burning of forest vegetation with no visible human conversion or agricultural activity afterward”. Uncertainty corresponds to the 95% confidence interval. Uncertainty is approximate for “urbanization” as the source reports an ambiguous error of “ $\pm <1\%$ ”.	
N	SEA LEVEL RISE	
	added water = $1.97 (+0.36, -0.34) \text{ mm / yr}$	<a href="#">HuID: 97108</a>
	thermal expansion = $1.19 (+0.25, -0.24) \text{ mm / yr}$	<a href="#">HuID: 97688</a>
	total observed sea-level rise = $3.35 (+0.47, -0.24) \text{ mm / yr}$	<a href="#">HuID: 81373</a>
	<b>Data Source(s):</b> Table 1 of Frederikse et al. 2020. DOI: <a href="https://doi.org/10.1029/2018MS001269">10.1029/2018MS001269</a> . <b>Notes:</b> Values correspond to the average global sea level rise of the years 1993 – 2018. “Added water” (barystatic) change includes effects from meltwater from glaciers and ice sheets, and changes in the amount of terrestrial water storage. Thermal expansion accounts for the volume change of water with increasing temperature. Values of “added water” and “thermal expansion” come from modeling. Total sea level rise is the observed value using a combination of measurement methods. “Other sources” reported on page 1 accounts for observed residual sea level rise not attributed to a source in the model. Values in parentheses correspond to the upper and lower bounds of the 90% confidence interval.	
O	POWER FROM FOSSIL FUELS	
	natural gas = $4.2 - 4.8 \text{ TW}$	<a href="#">HuID: 49947, 86175</a>
	oil = $6.0 - 6.5 \text{ TW}$	<a href="#">HuID: 4121, 39756</a>
	coal = $5.0 - 5.5 \text{ TW}$	<a href="#">HuID: 10400, 60490</a>
	total = $15.1 - 16.5 \text{ TW}$	<a href="#">HuID: 29470, 29109</a>
	<b>Data Source(s):</b> bp Statistical Review of World Energy, 2020. U.S. Energy Information Administration, 2020. <b>Notes:</b> Values are self-reported by countries. values from bp Statistical Review correspond to 2019 whereas values from the EIA correspond to 2018 estimates. Reported values of TW are computed from primary energy units assuming uniform use throughout the year. Oil volume includes crude oil, shale oil, oil sands, condensates, and natural gas liquids separate from specific natural gas mining. Natural gas value excludes gas flared or recycled and includes natural gas produced for gas-to-liquids transformation. Coal value includes 2019 value exclusively for solid commercial fuels such as bituminous coal and anthracite, lignite and subbituminous coal, and other solid fuels. This includes coal used directly in power production as well as coal used in coal-to-liquids and coal-to-gas transformations.	
P	POWER FROM RENEWABLE RESOURCES	
	wind = $0.32 - 0.38 \text{ TW}$	<a href="#">HuID: 30581, 85919</a>
	solar = $0.12 - 0.20 \text{ TW}$	<a href="#">HuID: 99885, 58303</a>
	hydroelectric = $1.2 \text{ TW}$	<a href="#">HuID: 15765, 50558</a>
	total renewable power = $1.9 \text{ TW}$	<a href="#">HuID: 75741, 20246</a>
	<b>Data Source(s):</b> bp Statistical Review of World Energy, 2020. U.S. Energy Information Administration, 2020. <b>Notes:</b> Reported values correspond to estimates for the 2017 calendar year. Renewable resources are defined as wind, geothermal, solar, biomass and waste. Hydroelectric, while presented here, is not defined as a renewable in the bp dataset. All values are reported as input-equivalent energy, meaning the input energy that would have been required if the power was produced by fossil fuels. BP reports that fossil fuel efficiency used to make this conversion was about 40% in 2017.	
M	FOSSIL FUEL EXTRACTION	
	volume of natural gas = $(3.9 - 4.0) \times 10^{12} \text{ m}^3 / \text{yr}$	<a href="#">HuID: 11468, 20532</a>
	volume of oil = $(5.5 \pm 5.8) \times 10^9 \text{ m}^3 / \text{yr}$	<a href="#">HuID: 66789, 97719</a>
	mass of coal = $(7.8 - 8.1) \times 10^{12} \text{ kg / yr}$	<a href="#">HuID: 78435, 48928</a>
	<b>Data Source(s):</b> bp Statistical Review of World Energy, 2020. U.S. Energy Information Administration, 2020. <b>Notes:</b> Oil volume includes crude oil, shale oil, oil sands, condensates, and natural gas liquids separate from specific natural gas mining. Natural gas value excludes gas flared or recycled and includes natural gas produced for gas-to-liquids transformation. Coal value includes solid commercial fuels such as bituminous coal, anthracite, lignite, subbituminous coal, and other solid fuels. All values from bp Statistical Review correspond to 2019 whereas values from the EIA correspond to 2018 estimates.	
R	OCEAN WARMING	
	heat uptake by ocean $\approx 346 \pm 51 \text{ TW}$	<a href="#">HuID: 94108</a>
	upper ocean ( $0 - 700 \text{ m}$ ) warming $\approx (5.9 \pm 0.4) \times 10^{-3} \text{ }^\circ\text{C / yr}$	<a href="#">HuID: 51068</a>
	<b>Data Source(s):</b> Table S1 of Cheng et al. 2017. doi: <a href="https://doi.org/10.1126/sciadv.1601545">10.1126/sciadv.1601545</a> . <b>Notes:</b> Values reported are averages over the time period 1992–2015. Uncertainties correspond to the 95% confidence intervals. Temperature change is considered in the upper 700 m because sea surface temperatures have high decadal variability and are a poor indicator of ocean warming; see Roemmich et al. 2015, doi: <a href="https://doi.org/10.1038/NCLIMATE2513">10.1038/NCLIMATE2513</a> .	

S	POWER FROM NUCLEAR FISSION	
	nuclear power = $0.75 - 0.87 \text{ TW}$	<a href="#">HuID: 48387</a>
	<b>Data Source(s):</b> bp Statistical Review of World Energy, 2020. U.S. Energy Information Administration, 2020. <b>Notes:</b> Values are self-reported by countries and correspond to estimates for 2017 calendar year. Values are reported as ‘input-equivalent’ energy, meaning the energy that would have been needed to produce a given amount of power if the input were a fossil fuel. This is calculated by multiplying the given power by a conversion factor representing the efficiency of power production by fossil fuels. In 2017, this factor was about 40%.	
T	NUCLEAR FALLOUT	
	anthropogenic $^{239}\text{Pu}$ and $^{240}\text{Pu}$ from weapons testing $\approx 1.4 \times 10^{11} \text{ kg / yr}$	<a href="#">HuID: 42526</a>
	<b>Data Source(s):</b> Table 1 in Hancock et al. 2014 doi: <a href="https://doi.org/10.1144/SP395.15">10.1144/SP395.15</a> . Fallout in activity from UNSCEAR 2000 Report on Sources and Effects of Ionizing Radiation Report to the UN General Assembly -- Volume 1. <b>Notes:</b> The approximate mass of Plutonium isotopes $^{239}\text{Pu}$ and $^{240}\text{Pu}$ released into the atmosphere from the $\approx 500$ above-ground nuclear weapons tests conducted between 1945 and 1980. Naturally occurring $^{239}\text{Pu}$ and $^{240}\text{Pu}$ is rare meaning that nearly all contemporary labile plutonium comes from human action.(Taylor 2001,doi: <a href="https://doi.org/10.1016/S1569-4860(01)80003-6">10.1016/S1569-4860(01)80003-6</a> ) The sum total mass of radionuclides released is $\approx 3300 \text{ kg}$ with a combined radioactive fallout of $\approx 11 \text{ PBq}$ . These values do not represent the globally distributed mass (excluding close-in fallout at some testing sites) and do not account for non-weapons sources.	
U	CONTEMPORARY EXTINCTION	
	animal species extinct since 1500 $> 750$	<a href="#">HuID: 44641</a>
	plant species extinct since 1500 $> 120$	<a href="#">HuID: 86866</a>
	<b>Data Source(s):</b> The IUCN Red List of Threatened Species. Version 2020-2. <b>Notes:</b> Values correspond to absolute lower-bound measurements of extinctions caused over the past $\approx 520$ years. Of the predicted $\approx 8$ million animal species, the IUCN databases catalogues only $\approx 900,000$ with only $\approx 75,000$ being assigned a conservation status. Representation of plants and fungi is even more sparse with only $\approx 40,000$ and $\approx 285$ being assigned a conservation status, respectively. The number of extinct animal species is undoubtedly higher than these reported values, as signified by an inequality symbol ( $>$ ).	
M	EARTH MOVING	
	waste and overburden from coal mining $\approx 6.5 \times 10^{13} \text{ kg / yr}$	<a href="#">HuID: 72899</a>
	earth moved from urbanization $> 1.4 \times 10^{14} \text{ kg / yr}$	<a href="#">HuID: 59640</a>
	<b>Data Source(s):</b> Supplementary table 1 of Cooper et al. 2018. DOI: <a href="https://doi.org/gfwhd">doi.org/gfwhd</a> . <b>Notes:</b> Coal mining waste and overburden mass is calculated given commodity-level stripping ratios (mass of overburden/waste per mass of coal resource mined) and reported values of global coal production by type. Urbanization mass is presented as a lower bound estimate of the mass of earth moved from global construction projects. This comes from a conservative estimate that the ratio of the mass of earth moved per mass of cement/concrete used in construction globally is 2:1. This value is highly context dependent and we encourage the reader to read the source material for a more thorough description of this estimation.	
	erosion from agricultural land $> 1.2 - 2.4 \times 10^{13} \text{ kg / yr}$	<a href="#">HuID: 19415, 41496</a>
	<b>Data Source(s):</b> Pg. 377 of Wang and Van Oost 2019. DOI: <a href="https://doi.org/10.1177/0959683618816499">10.1177/0959683618816499</a> . Pg. 21996 of Borrelli et al. 2020 DOI: <a href="https://doi.org/10.1073/pnas.2001403117">10.1073/pnas.2001403117</a> . <b>Notes:</b> Cumulative sediment mass loss over history of human agriculture due to accelerated erosion is estimated to be $\approx 30,000 \text{ Gt}$ . Recent years have an estimated erosion rate ranging from $12 \text{ Pg / yr}$ (Wang and Van Oost) to $\approx 24 \text{ Pg / yr}$ (Borrelli et al.). Values come from computational models conditioned on time-resolved measurements of sediment deposition in catchment basins.	
	ACKNOWLEDGMENTS	
	We are incredibly grateful for the generosity of a wide array of experts for their advice, suggestions, and criticism of this work. <b>No specific order, thank the following:</b> Joel Cohen, Alon Shepon, Eric Galbraith, Sean B. Carroll, Justin Bois, Shyam Saladi, APh150c course, Wati Taylor, Dan Fisher, Gidon Eshel, Greg Huber, Michelle Dan, Brad Marston, Hamza Ranjwala, Ken Caldeira, Tapio Schneider, Pietro Perona, Paul Falkowski, Stephen Quake, John Grotzinger, Benjamin Rubin, Bethany Ehlmann, Ned Wingreen, Matthew Burgess, Lea Goentoro, Neil Fromer, Thomas Rosenbaum, Arthur Smith, Dianne Newman, Victoria Orphan, Eliot Meyerowitz, Yue Qin for providing data on water consumption. Suzy Beeler, Soichi Hirokawa, Manuel Razo-Mejia and all members of the Phillips lab at Caltech. This work was supported by the Resnick Institute for Sustainability at the California Institute of Technology.	